Microstructure and Mechanical Properties of Friction Stir Weld of Dissimilar Ti6Al4V Titanium Alloy to AA2024 Aluminum Alloy

Yuhua Chen, Wenming Cao, Shuhan Li, Chao Chen and Jilin Xie

Abstract Dissimilar Ti6Al4V titanium alloy and AA2024 aluminum alloy sheets with a thickness of 3 mm were friction stir welded successfully, and the microstructure and mechanical properties of the butt joints were investigated. The results show that: the stirred zone (SZ) exhibits a mixture structure, which is characterized by fine recrystallized grains of aluminum alloy and titanium particles. Unfilled defects are observed among titanium particles in SZ. Moreover, at the aluminum side the thermal-mechanically affected zone (TMAZ) and the heat affected zone (HAZ) appeared like in the traditional FSW-joints. But, at the titanium side, a recrystallization band with a width of 6–10 μm and a layer with fibrous structures are found at the joint interface. Also, the Ti–Al compounds layer with some micro-cracks is presented in the fibrous structure. The hardness distribution of the joint along the cross-section centerline varies significantly due to the existence of different broken titanium particles. The ultimate tensile strength (UTS) of the joint reached 83% of aluminum base metal and the joint failed with a ductile–brittle fracture mode.

Keywords Ti/Al dissimilar metals · FSW · Microstructure
Mechanical properties

1 Introduction

Compared with other materials, titanium alloys have many advantages such as low density, high specific strength, and excellent corrosion-resistance, so they are widely used in automotive, aerospace, and ship industries. Aluminum alloys are also attractive in these fields due to their low density and good economic features. In order to meet the special performance requirements for aviation materials,

Y. Chen (✉) · W. Cao · S. Li · C. Chen · J. Xie
School of Aeronautical Manufacturing Engineering, Nanchang Hangkong University, Nanchang, China
e-mail: ch.yu.hu@163.com

S. Chen et al. (eds.), *Transactions on Intelligent Welding Manufacturing*,
Transactions on Intelligent Welding Manufacturing,
https://doi.org/10.1007/978-981-10-7043-3_11

structures with high strength and low weight are widely used. The joining of titanium alloy with aluminum alloy could have a major application in aerospace and automobile industries where high strength and low weight are desirable. However, it is difficult to weld these two alloys because of the great differences in physical, chemical, and metallurgical properties [1–4]. Some welding methods for joining these two materials such as laser and hybrid laser welding [5–8], solid-state diffusion bonding [9, 10], ultrasonic welding [11, 12], as well as explosive welding [13, 14] have been reported.

These studies show that the key issue encountered in welding Al alloys to Ti alloys is the formation of intermetallic compounds in joints. Friction stir welding (FSW) is a novel solid-state welding technology [15]. It is suitable for welding Al alloys to Ti alloys due to the lower temperature and shorter time (compared to the fusion welding process) during the process [16–20].

Although there are a few studies about friction stir welding of Ti/Al dissimilar alloys, the details of the microstructural evolution of dissimilar joints have not been fully understood and the ultimate tensile strength of the joint still cannot meet the industry demand.

In this paper, AA2024 alloy and Ti6Al4V alloy, which are widely used in industries, are welded by FSW. To make a comprehensive analysis of the joining mechanism, the microstructure, intermetallic compounds, hardness distribution, and tensile strength of the dissimilar joints are investigated.

2 Experiment Details

The experiment materials are 3 mm thick of AA2024 alloy and Ti6Al4V alloy plates with the chemical compositions shown in Tables 1 and 2, respectively.

The butt joints were welded using an FSW tool consisting of a threaded pin of 6 mm diameter and a concave shoulder of 18 mm diameter. The welding tool was made from nickel base superalloy. The processing parameters were selected as 700 rpm for tool rotation speed and 60 mm/min for travel speed based on the large number of experiments. A schematic illustration of the dissimilar FSW experiment was shown in Fig. 1. During FSW process, Ti6Al4V and AA2024 were placed at the advancing side (AS) and the retreating side (RS) of the tool pin, respectively. The pin was inserted into the AA2024 aluminum sheet with 2.5 mm offset to the welding line. The weld sections taken perpendicular to the welding direction were polished and etched using different kind of etchant (1% HF + 3% HNO_3 + 5% H_2O to Al and 3% HF + 10% HNO_3 + 87% H_2O to Ti). Polished metallographic cross sections were examined by optical microscopy (OM) and scanning electron

Table 1 Chemical composition of AA2024

Cu	Si	Mn	Mg	Fe	Zn	Ni	Ti	Al
4.3	1.0	0.73	0.55	0.3	0.08	0.02	0.02	Balance

Table 2 Chemical composition of Ti6Al4V

Al	V	Fe	C	N	H	O	Ti
6.0	4.0	0.026	0.015	0.008	0.007	0.06	Balance

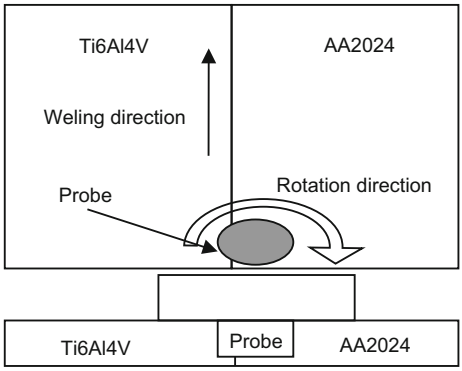

Fig. 1 Schematic illustration showing setup of dissimilar FSW

microscope (SEM) equipped with an EDX system. Hardness tests were done every 500 μm at the center of the section using a Vickers indenter at a load of 0.2 kg. Tensile tests were conducted at a crosshead speed of 1 mm/min.

3 Results and Discussions

3.1 Macrostructure and Microstructure of Dissimilar Joint

Since the hardness and melting point of the Ti6Al4V alloy are higher than those of the AA2024 alloy. In dissimilar FSW, the alumina alloys should have better plastic flowability due to the welding temperature is not enough to plasticizing the Ti6Al4V alloy. By in terms of the pin offset technique, Al–Ti dissimilar joints can be formed. However, it is hard to join the two metals if the pin totally inserted to the alumina with an offset of 3 mm in this study. Figure 2 shows the surface morphology of the dissimilar welded specimen. The surface of the joint is very smooth and covered by a layer of aluminum alloy. Curved key sheaths produced by tool shoulder were not very clear. Figure 3 shows the cross-sectional macrostructure of the dissimilar weld. Because the welding tool was shifted toward the Al alloy, the stir zone (SZ) occurs mainly on the Al side of the joint. The stir zone is composed by Al and Ti, and an onion ring like structure was formed at the bottom of the joint. The interface between the nugget zone and the Ti base metal is not very straight, two hook structures are observed at the top and the bottom of the joint, respectively. They were believed to enhance the joints tensile strength capacity. No pore or other defect can be found in Figs. 2 and 3, indicating that sound joint could be produced with the designated experimental parameters.

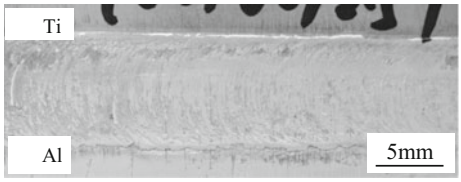

Fig. 2 Appearances of dissimilar joint

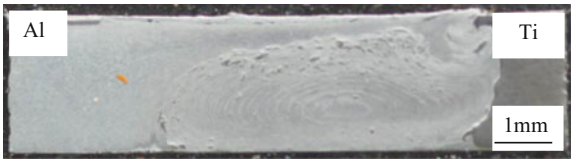

Fig. 3 Cross-section structure of dissimilar joint prepared by FSW

Figure 4 shows the optical microstructures of the dissimilar joint. On the retreating side, there are SZ, TMAZ, and HAZ. While at the advancing side of the joint, there are no obvious SZ, TMAZ, and HAZ, because the melting point of titanium alloy is higher than that of the aluminum alloy. As shown in Fig. 4a, the microstructure of aluminum BM is a typical quenching and nature aging structure which is mainly composed of aluminum matrix and precipitation strengthening phases. Figure 4b shows the microstructure of titanium BM, which is a mixture of α and β phases. Figure 4c shows the microstructures of HAZ and TMAZ in the Al side. No plastic deformation occurred in HAZ, but the grains in HAZ were heated to growing up during FSW. Compared with the microstructures of the BM, it could be seen that the grain shape in HAZ does not change, but the size becomes coarse due to the thermal cycle in the welding process. Meanwhile, grains in the TMAZ show a curved shape, indicating that these grains undergo notable plastic deformation caused by the welding tool. Figure 4d shows the interface between the aluminum alloy and titanium alloy; also it is the interface of stir zone and advancing side. There is a hook structure inserting into the SZ firmly hooking the aluminum substrate. During the welding process, titanium alloy was strongly scratched by the rotation tool. And parts of titanium were separated from the substrate turn to titanium particles flowing with the plastic aluminum; hook structure was the titanium that not separated completely. All means that the titanium at the interface undergoes intensively plastic deformation by the tool. Figure 4e and f show the SZ of the dissimilar joint. Figure 4e is the weld nugget besides the TMAZ in aluminum side. Due to the dynamic recrystallization caused by welding tool, grains in this zone are fine grains and obviously streamlined organization; also part of titanium particles was observed in this area. Figure 4f shows large number of different forms titanium particles embedded in the aluminum alloy matrix, and also with many unfilled flaws between the adjoining titanium particles. The reason for the defects formed is that the gap formed by two particles is too small to be filled by the plastic aluminum alloys during the weld processing. Microstructures in the SZ are very complicated and aluminum grains size in this region is not even, grains besides the particle are smaller than those of far from it. However, they are all smaller than those of the region where no titanium particles exist.

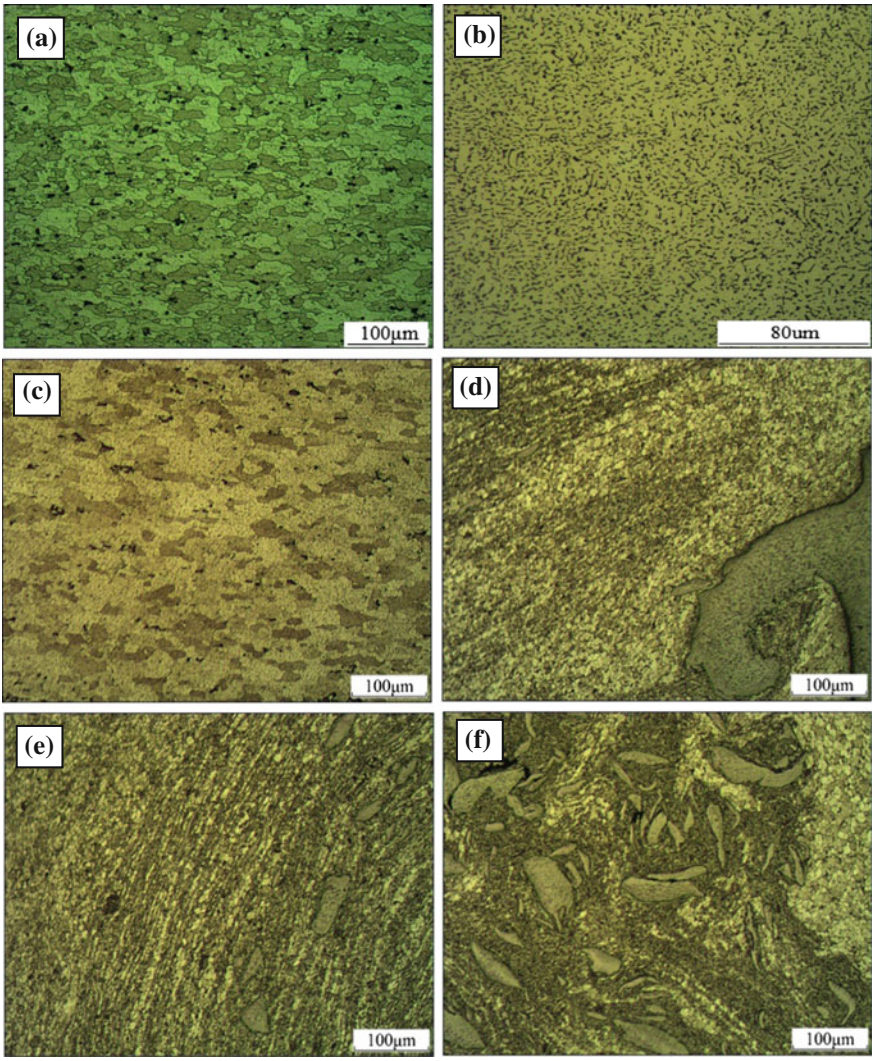

Fig. 4 Optical microstructures of the dissimilar joint: **a** Aluminum base metal; **b** Titanium base metal; **c** HAZ and TMAZ in Al side; **d** interface of Al/Ti; **e** SZ near the Al side; **f** SZ near the Ti side

3.2 Interface Characteristic of Dissimilar Joints

Figures 5a–d is the interface between the stir zone (SZ) and the Ti alloy side. Figure 5e is the EDS test result of area M in Fig. 5c and f is micro-XRD test result. It can be clearly seen from Fig. 5a that there are some titanium particles in the figure, embedded in the aluminum matrix, the dark part, with different size and

shapes. Moreover, the titanium particles present flow patterns with the aluminum alloy matrix. Nevertheless, in Fig. 5a layer of fibrous structure that is not the same as the two parent materials is observed.

This layer is considered to be the diffusion area because the EDS test result and the micro-XRD test result show that Ti–Al components were formed in this area. The EDS test result shows that elements in Ti alloy and elements in Al alloy are

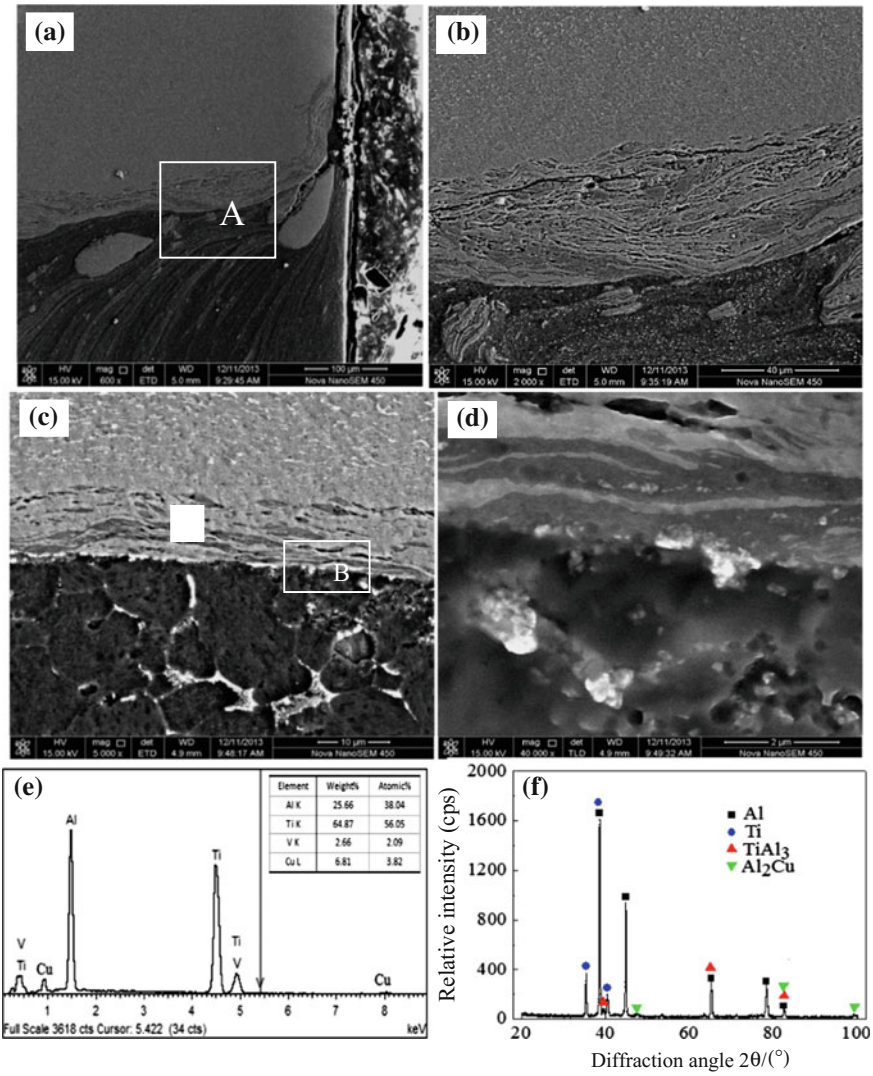

Fig. 5 SEM picture of the joint interface: **a** Upper area of the interface; **b** amplification of zone A in (a); **c** middle area of the interface; **d** amplification of zone B in figure (c); **e** EDS test of zone M in (c); **f** micro-XRD test of interface

diffusion to each other in this area formed intermetallic compounds (IMC) $TiAl_3$ as shown in the micro-XRD test result. Further, amplification of the interface as shown in Fig. 5c, a narrow band adjacent to the fibrous structure is observed in the titanium parent, where the equiaxed primary α and β grains have been elongated.

The width of this band is about 6–10 μm. Disappearance of remaining lamellar structures that have been found in the titanium alloy corroborates recrystallization in the small affected band. The fibrous structure shown in Fig. 5d is a very complicated structure that the titanium alloy and IMC layers appear alternately as lamellar-structure. Besides, some micro-cracks are found in the IMC layers.

3.3 Mechanical Properties of Dissimilar Joints

As shown in Fig. 6, the hardness level continuously amounts to 120 HV0.2 on the aluminum side. A sharp increase to approximately 330 HV0.2 occurs at the Ti/Al transition. Hardness values dramatic changes in the SZ. In spite of the high FSW process temperature, hardness values in the center of the SZ reach 150 HV0.2. Probably, this is a result of grain boundary hardening. Individual higher hardness values (shown point P) occurred in the SZ near the HAZ which occurred when the indenter hit a titanium particle. On that level, the hardness profile is proceeding on the retreating side in principle like in conventional FSW-joints, except, the loss in hardness to aluminum of 90 HV0.2 is caused by the relatively high heat input, which leads to an over-aging effect. The ultimate tensile strength (UTS) of the dissimilar joint is 347 MPa that is representing 83% of the UTS of 2024 base material. Figure 7 shows the fracture location of the dissimilar joint. It can be seen that the fracture location is between the SZ and the aluminum alloy side.

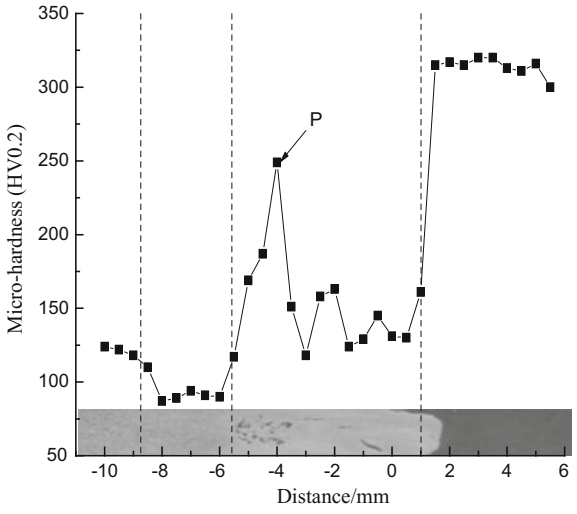

Fig. 6 Micro-hardness distribution of titanium/aluminum FSW joint

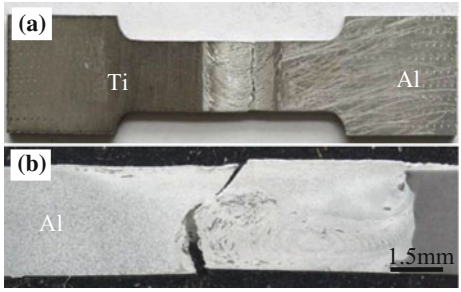

Fig. 7 Specimen after the tensile test: **a** Top surface of tensile specimen; **b** optical image of a cross-section of joint

Furthermore, the failed location was along the 45° direction with respect to the weld specimen surface at the crown, then, turn to about 90° at the bottom. The unfilled defects between the titanium particles as mentioned above were the main reason to explain the fracture direction turned.

Figure 8 illustrates the SEM images of the tensile fracture surface. Figure 8a shows the appearance of tensile fracture and the fracture features vary appreciably with the locations across the weld due to the complex microstructures of the nugget. Figures 8b–d show the magnified micrographs of the fracture surfaces marked in Fig. 8a. As shown in Fig. 8b, flat surface and small dimples can be observed in this region. Intergranular fracture patterns exist in some regions, as shown in Fig. 8c and some cleavage planes can be seen clearly in the region. A large number of dimples with different depth are observed in Fig. 8d, indicating that a ductile fracture has taken place in these regions. Therefore, the fracture mode of the dissimilar joints can be defined as a ductile–brittle mixed fracture.

4 Conclusion

Friction stir welding of Ti6Al4V alloy and AA2024 alloy with a thickness of 3 mm was conducted. The macro/microstructure, the interface characteristic, and the mechanical properties of the dissimilar joint were investigated. The results can be summarized as follows.

1. AA2024 aluminum alloy and Ti6Al4V titanium alloy are joined successfully through FSW with pin offset technique under a rotation speed of 700 r/min and a welding speed of 60 mm/min.
2. TMAZ and HAZ occurred at the aluminum side like in the conventional FSW-joints. Unfilled defects are observed at the SZ. Grains near the titanium particle are smaller than those of far from it. However, they are all smaller than those of the zone where no titanium particles exist.
3. At the titanium side, a recrystallization band with a width of 6–10 μm and a layer of fibrous structure are observed. The Ti–Al compounds layer, including $TiAl_3$, are formed in the fibrous structure, and also some micro-cracks are found in the IMC layers.

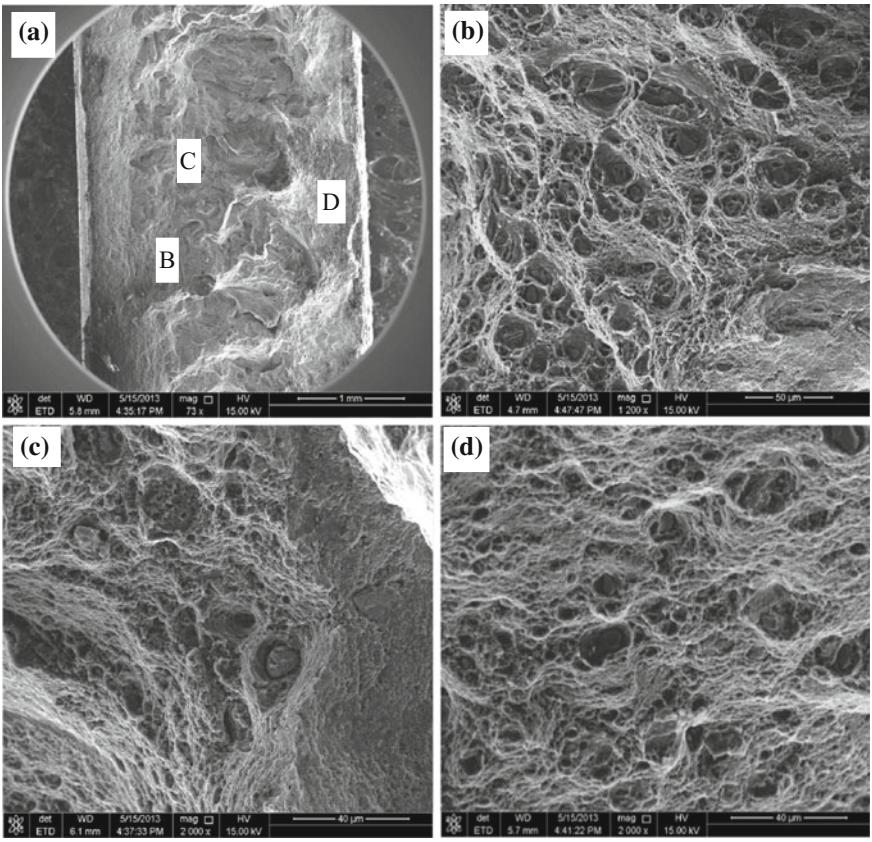

Fig. 8 Fracture surface from titanium alloy side of the joint: **a** Overview of the surface; **b** zone B; **c** zone C; **d** zone D

4. The hardness of the joint is sharply changed. Sudden drop from average hardness of 330 HV at titanium alloy to average hardness of 120 HV at aluminum side. The hardness of the forging organization in the SZ was higher than that of the base metal by 150 HV and the enriched titanium particles regional owns a hardness level peak during the SZ. The average hardness of 90 HV occurred at HAZ. The UTS of the joint is 347 MPa which is 83% of the AA2024 alloy and the joints failed with a ductile–brittle fracture mode.

Acknowledgements The National Natural Science Foundation of China (51265042), the Science and Technology Planning Project of Jiangxi Province (20171BCB24007), and the Natural Science Foundation of Jiangxi Province (20114BAB206006).

References

1. Mishrar RS, Ma ZY (2005) Friction stir welding and processing. Mater Sci Eng R 50:1–78
2. Kenevisi MS, Khoie SMM, Alaei M (2013) Microstructural evaluation and mechanical properties of the diffusion bonded Al/Ti alloys joint. Mech Mater 64(1):69–75
3. Samavatian M, Khodabandeh A, Halvaee A et al (2015) Transient liquid phase bonding of Al 2024 to Ti-6Al-4V alloy using Cu-Zn interlayer. Trans Nonferrous Met Soc China 25(3): 770–775
4. Tomashchuk I, Sallamand P, Cicala E et al (2015) Direct keyhole laser welding of aluminum alloy AA5754 to titanium alloy Ti6Al4V. J Mater Process Technol 217:96–104
5. Chen SH, Li LQ, Chen YB et al (2010) Si diffusion behavior during laser welding-brazing of Al alloy and Ti alloy with Al-12Si filler wire. Trans Nonferrous Met Soc China 20(1):64–70
6. Vaidya WV, Horstmann M, Ventzke V et al (2010) Improving interfacial properties of a laser beam welded dissimilar joint of aluminum AA6056 and titanium Ti6Al4V for aeronautical applications. J Mater Sci 45:6242–6254
7. Song ZH, Kazuhiro N, Wu AP et al (2013) Interfacial microstructure and mechanical property of Ti6Al4V/A6061 dissimilar joint by direct laser brazing without filler metal and groove. Mater Sci Eng A 60:111–120
8. Casalino G, Mortello M, Peyre P (2015) Yb–YAG laser offset welding of AA5754 and T40 butt joint. J Mater Process Technol 223:139–149
9. Yao W, Wu AP, Zou GS (2007) Structure and forming process of the Ti/A1 diffusion bonding joints. Rare Metal Mater Eng 36(4):700–704
10. Chen SH, Li LQ, Chen YB et al (2011) Joining mechanism of Ti/Al dissimilar alloys during laser welding-brazing process. J Alloy Compd 509(3):891–898
11. Zhang CQ, Robson JD, Ciuca O et al (2014) Microstructural characterization and mechanical properties of high power ultrasonic spot welded aluminum alloy AA6111-TiAl6V4 dissimilar joints. Mater Charact 97:83–91
12. Zhu Z, Kang YL, Wang X (2012) Ultrasonic welding of dissimilar metals AA6061 and Ti6Al4V. Int J Adv Manuf Technol 59(5):569–574
13. Xia HB, Wang SG, Ben HF (2014) Microstructure and mechanical properties of Ti/Al explosive cladding. Mater Des 56:1014–1019
14. Samavatian M, Halvaee A, Amadeh AA et al (2014) An investigation on microstructure evolution and mechanical properties during liquid state diffusion bonding of Al2024 to Ti-6Al-4V. Mater Charact 98(13):113–118
15. Thomas WM, Nicholas ED, Needham JC, et al (1991) GB Patent 9125978, 8 December 1991
16. Wu AP, Song ZH, Kazuhiro N et al (2015) Interface and properties of the friction stir welded joints of titanium alloy Ti6Al4V with aluminum alloy 6061. Mater Des 71:85–92
17. Bang HS, Song HJ et al (2013) Joint properties of dissimilar Al6061-T6 aluminum alloy/Ti6%Al4%V titanium alloy by gas tungsten arc welding assisted hybrid friction stir welding. Mater Des 51:544–551
18. Li B, Zhang ZH, Shen YF et al (2014) Dissimilar friction stir welding of Ti–6Al–4V alloy and aluminum alloy employing a modified butt joint configuration: influences of process variables on the weld interfaces and tensile properties. Mater Des 53:838–848
19. Aonuma M, Nakata K (2011) Dissimilar metal joining of 2024 and 7075 aluminum alloys to titanium alloys by friction stir welding. Mater Trans 52(5):948–952
20. Chen YH, Ni Q, Ke LM (2012) Interface characteristic of friction stir welding lap joints of Ti/Al dissimilar alloys. Trans Nonferrous Met Soc China 22(2):299–304